Trends in Analytical Chemistry 118 (2019) 19–28

Contents lists available at ScienceDirect

Trends in Analytical Chemistry

journal homepage: www.elsevier.com/locate/trac

# Flow field-flow fractionation: Recent applications for lipidomic and proteomic analysis☆

Myeong Hee Moon*

*Department of Chemistry, Yonsei University, 50 Yonsei-ro, Seoul, 03722, Republic of Korea*

ARTICLE INFO

*Article history:*
Available online 23 May 2019

*Keywords:*
Flow field-flow fractionation (FlFFF)
Mass spectrometry
Proteomics
Lipidomics
Metalloproteins

ABSTRACT

Flow field-flow fractionation (FlFFF) is a versatile size-based separation method suitable for biological macromolecules including proteins/protein aggregates, DNA, subcellular organelles, extracellular species, and whole cells. This review introduces briefly the basic principles of FlFFF and its recent applications for proteomic and lipidomic analysis, which are described in two parts: (1) off-line coupling of FlFFF with MS and other bioanalytical methods, and (2) on-line FlFFF with MS. The first part includes applications for lipoproteins, exosomes, and subcellular organelles for the size-dependent analysis of proteins and lipids in narrow size-fractions collected during FlFFF, followed by independent analysis including western blotting and nanoflow liquid chromatography-electrospray ionisation-tandem mass spectrometry (nLC-ESI-MS/MS). The second part highlights the on-line FlFFF-MS, in which a miniaturised FlFFF channel is coupled to ESI-MS/MS for the high-speed lipid analysis of lipoproteins and to inductively-coupled plasma MS for the direct analysis of metals in metalloproteins from blood plasma.



## 1. Introduction

Research in the life sciences is expanding rapidly, and there has been increasing interest in improving human health and life expectancy. Particularly, proteomics, metabolomics, and lipidomics researches are focused on understanding the relationship between the structures and functions of biologically active species at molecular, subcellular, and extracellular levels. Omics researchers are also pursuing the development of potential biomarkers that can be utilised for the diagnosis and prognosis of diseases. However, research in these fields involves isolation or purification of active components from complex biological mixtures. Therefore, selective isolation/separation or purification of complicated biological samples is a prerequisite step for omics research, regardless of whether highly efficient analytical or assay methods are available.

There are several methods for isolation or purification of biological macromolecular species. Cellular and subcellular species are traditionally isolated using centrifugation methods, which are simple but time-consuming and make it difficult to achieve pure fractions [1,2]. Affinity-based purification provides highly selective purification of organelles using antibodies with a specific affinity for certain proteins [1,3]. Fluorescence-activated cell sorting (FACS) performs the separation of live cells based on staining using fluorophore-conjugated antibodies [4]. Both techniques provide high efficiency in the selective isolation of cells or organelles, but require specific antibodies, which are limited.

Lipoproteins or proteins are purified using density gradient ultracentrifugation (DGU) [5–7], polyacrylamide gel electrophoresis (PAGE) [8,9], and size exclusion chromatography (SEC) [10]. While DGU and PAGE provide accurate fractions based on density and size, respectively, DGU requires considerable amounts of sample and PAGE requires retrieval of target materials trapped in gels. SEC offers fast and reproducible separation, but the possible interaction of sample components with packing materials cannot be completely avoided. Separating proteins using chromatographic methods often induces a loss of molecular conformation or dissociation of protein subunits, and in some cases, the loss of metal ions from metal-containing proteins. Because each of these methods has several advantages along with some disadvantages, the need for a versatile separation method continues to grow.

## 2. Flow field-flow fractionation (FlFFF)

FlFFF is an elution-based method for the separation and characterisation of macromolecules, including nanoparticles and

☆ This invited contribution is dedicated to the 70th anniversary of Dalian Institute of Chemical Physics, Chinese Academy of Sciences.

* Fax: +82 2 364 7050.
*E-mail address:* mhmoon@yonsei.ac.kr.

https://doi.org/10.1016/j.trac.2019.05.024
0165-9936/

**Abbreviations**

| | |
|---|---|
| 2D-PAGE | two-dimensional polyacrylamide gel electrophoresis |
| ACS | acute coronary syndrome |
| AD | Alzheimer's disease |
| AF4 | asymmetrical flow field-flow fractionation |
| ApoA1 | apolipoprotein A1 |
| CAD | coronary artery disease |
| CID | collision induced dissociation |
| DG | diacylglycerol (or DAG) |
| DGU | density gradient ultracentrifugation |
| DRI | differential refractive index |
| ESI | electrospray ionisation |
| FACS | fluorescence-activated cell sorting |
| FFF | field-flow fractionation |
| FI-AF4 | frit inlet asymmetrical flow field-flow fractionation |
| FLD | fluorescence detector |
| FlFFF | flow field-flow fractionation |
| HDL | high-density lipoprotein |
| HF5 | hollow fiber flow field-flow fractionation |
| ICPMS | inductively coupled plasma mass spectrometry |
| LDL | low-density lipoprotein |
| LPC | lysophosphatidylcholine |
| LPS | lysophosphatidylserine |
| mAF4 | miniaturised AF4 |
| MALS | multiangle light scattering |
| MCI | mild cognitive impairment |
| MMSE | mini-mental state examination |
| MxHF5 | multiplexed hollow fiber flow field-flow fractionation |
| MS | mass spectrometry |
| MVB | multivesicular body |
| nLC-ESI-MS/MS | nanoflow liquid chromatography-electrospray ionisation-tandem mass spectrometry |
| nUHPLC | nanoflow ultrahigh performance liquid chromatography |
| Ox-PL | oxidized phospholipid |
| PA | phosphatidic acid |
| PC | phosphatidylcholine |
| PCa | prostate cancer |
| PE | phosphatidylethanolamine |
| PEp | phosphatidylethanolamine plasmalogen |
| PI | phosphatidylinositol |
| PG | phosphatidyl glycerol |
| PL | phospholipid |
| PS | phosphatidylserine |
| SEC | Size exclusion chromatography |
| SEM | scanning electron microscopy |
| SM | sphingomyelin |
| SRM | selected reaction monitoring |
| TEM | transmission electron microscopy |
| TG | triacylglycerol (or TAG) |
| VLDL | very low-density lipoprotein |

biopolymers, by size difference [11–15]. Separation in FlFFF is carried out in an open channel space (either rectangular or cylindrical design) by the combination of two flow streams: migration flow moving along the channel axis and crossflow moving across the channel [11,13]. In a typical rectangular channel (Fig. 1), the crossflow moves perpendicular to the migration flow and drives sample components towards the channel wall and sample species travel away from the channel wall via diffusion, resulting in differential distributions against the wall according to differences in hydrodynamic size. This is achieved through the balance between the force created by crossflow and the force created by diffusion. Smaller particles or low molecular weight proteins with faster diffusion are placed at a higher equilibrium position above the channel wall than larger species, and thus, migrate faster when a migration flow with a parabolic flow velocity profile is applied [11]. Therefore, size-based separation in FlFFF is achieved by increasing order of hydrodynamic diameter, which is a typical mode of separation and is applicable to sample components less than 1 μm in diameter (Fig. 1a). Retention time ($t_r$) of a sample component in FlFFF is proportional to the Stoke's diameter ($d_s$) of particles or macromolecules and the ratio of crossflow rate ($\dot{V}_c$) to migration flow rate ($\dot{V}$):

$$t_r = \frac{\pi \eta w^2}{2kT} \frac{\dot{V}_c}{\dot{V}} d_s \quad (1)$$

where $\eta$ is the viscosity of the carrier liquid, $w$ is the channel thickness, and $kT$ is the thermal energy. However, particles above 1 μm in diameter are less prone to diffusion. Separation of supramicron-sized species like cells is achieved in an opposite elution order (steric/hyperlayer mode; Fig. 1b) because the centre of larger particles is exposed to a higher stream velocity of migration flow than that of smaller particles [16]. Because separation in FlFFF takes place in an unobstructed channel space using aqueous solutions, including a biocompatible buffer, it prevents unwanted interactions between sample components and the stationary

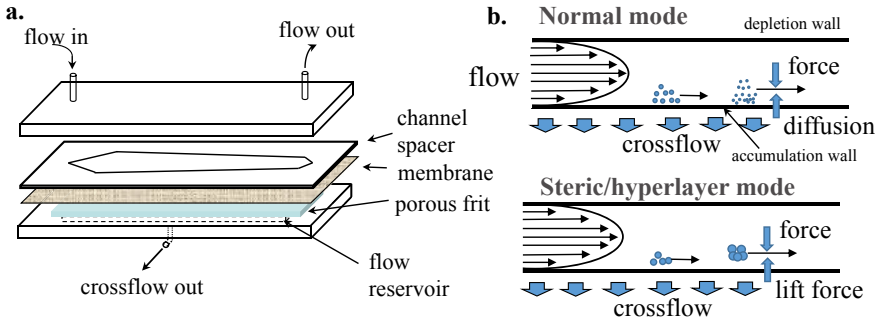


**Fig. 1.** (a) Structure of FlFFF channel with (b) elution profiles in normal mode and steric/hyperlayer mode.

phase, like those seen in chromatography. The biocompatible and soft nature of FlFFF has led to wide applications for various biological materials: proteins and protein aggregates [17–20], microRNA [21,22], protein-DNA interaction [23], exosomes [24–26], lipoproteins [27,28], organelles [29,30], cells [31,32], and virus-like particles [33,34].

A few variants in the FlFFF channel design exist. FlFFF was developed with a symmetrical channel geometry in which both of the channel walls that clamp the channel spacer were made with porous frit materials, so that crossflow was delivered from one wall of the channel to the other [35]. Subsequently, an asymmetrical channel design (Fig. 1a), in which the depletion wall was replaced with a plain wall, became widely utilised because the asymmetrical FlFFF (AF4) channel reduced the relaxation band-broadening of an initial sample zone [36,37]. Prior to separation in FlFFF, sample components must undergo the relaxation process, in which molecules are placed at equilibrium positions where two counter-directing forces (field and diffusion) are balanced. In symmetrical FlFFF, this is achieved by applying crossflow alone while migration flow is halted for some time. In AF4, relaxation is carried out by applying two flow streams through the inlet and outlet simultaneously at a ratio of 1:9 (referred to as focusing/relaxation) so that sample components are focused at the 1/10 position along the channel length. This results in a substantial decrease in the initial width of a sample zone. Moreover, migration flow rate in AF4 decreases along the channel axis, while that of the symmetrical channel is the same as the outflow rate ($\dot{V}_{out}$), leading to an additional decrease in the width of a migrating sample band. Both effects lead to the resolution enhancement of AF4 compared to symmetrical FlFFF. Due to the decrease in migration flow rate along the channel axis in AF4, $\dot{V}$ in Eq. (1) is replaced with

$$\dot{V} = \dot{V}_c \left[ \ln \left( \frac{\dot{V}_{in} - \frac{A(z)}{A_c}\dot{V}_c}{\dot{V}_{out}} \right) \right]^{-1} \qquad \text{(for an AF4 channel)} \qquad (2)$$

where $\dot{V}_{in}$ is the flow rate of the channel inlet, $A_c$ is the total area of the accumulation wall, and $A(z)$ is the area of the accumulation wall from the channel inlet to distance $z$ from the inlet, typically the focusing/relaxation point. The implementation of a 3-4 cm-long inlet frit at the beginning of the depletion wall of the AF4 channel allows for AF4 operation without the focusing/relaxation procedure, so that sample components entering the channel inlet are hydrodynamically pushed toward the accumulation wall by a high speed flow introduced to a small inlet frit. This is referred to as frit inlet-AF4 (FI-AF4) [38,39]. Since relaxation of sample components in FI-AF4 is achieved hydrodynamically without halting the migration flow, possible sample adsorption at the accumulation wall during stop-flow relaxation can be reduced [40], which facilitates the separation of ultra-high molecular weight species [41,42]. Another variant of FlFFF is hollow-fibre FlFFF (HF5), which uses a hollow fibre (HF) made of polymeric porous membrane as a separation channel [43,44]. In HF5, the radial flow exiting from the cylindrical membrane wall acts as the crossflow does in the rectangular channels, and the channel operation procedure is the same as that of AF4. Since HFs can be easily replaced, HF5 is suitable for disposable use when carryover of sample species is critical. Studies have shown that the performance of HF5 was comparable to that of AF4, aside from the low throughput. To increase throughput, several HF modules can be combined in parallel to assemble a multiplexed HF5 (MxHF5) for semi-preparative scale separation [45].

Detection in FlFFF is typically performed using (1) a UV detector for the turbidity measurement of most particulate and biological macromolecules, (2) DRI detector for most polymers, or (3) FLD for sample materials containing fluorophores. MALS detectors have been powerfully used in serial with UV or DRI detectors, which provide the molecular weight distribution and structural information for macromolecules. FlFFF effluent can be directly fed into MS via ESI for the on-line analysis of proteins/peptides and lipids, or via ICP for metal distributions in metalloproteins. The following sections will cover the recent applications of off-line and on-line hyphenation of FlFFF with independent analytical methods for the size-dependent proteomic and lipidomic analysis of biomacromolecules.

## 3. Off-line coupling of FlFFF with analytical methods

During an FlFFF run, biomacromolecules can be collected in intact condition into narrow size fractions for secondary analysis using available analytical and bioanalytical methods: SEM or TEM for morphological examination, western blotting for the confirmation of proteins with antibodies, 2D-PAGE for proteins, and nLC-ESI-MS/MS for proteomic and lipidomic analysis (Fig. 2a).

### 3.1. High-speed size sorting of subcellular organelles by FlFFF

Due to the biocompatible nature of FlFFF, utilising aqueous buffer solutions as a carrier liquid for separation, FlFFF has demonstrated its ability to separate cellular species such as whole bacterial cells, red blood cells, and subcellular components like mitochondria, for the determination of size distributions [29,31,32,46]. Because the diameters of cells are above a few micrometres, FlFFF can be utilised for high-speed size-based separation in the steric/hyperlayer elution mode in which larger cells elute earlier than smaller ones. However, for cell homogenates – which contain subcellular species like nuclei, mitochondria, lysosomes, and peroxisomes as well as proteins, of which sizes range from a few nanometres to a few microns – it is often difficult to isolate/purify subcellular species under a single run condition. Because organelles have their own distinct functions, and biologically active species, such as functional proteins related to pathologies or mRNAs, are often present at low abundance and in specific subcellular locations, abnormalities in the functions of specific organelles may be involved in the progression of diseases [47–49]. Therefore, selective isolation of subcellular species is a challenging task.

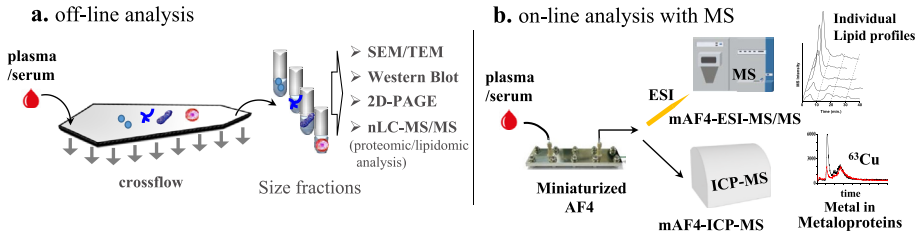


**Fig. 2.** Schematics of (a) off-line analysis of FlFFF with other analytical methods, and (b) on-line analysis of FlFFF and mass spectrometry.

FlFFF was utilised for the separation and isolation of subcellular species using a sequential separation of cell homogenates in steric/hyperlayer mode, followed by separation of the collected fraction in the normal mode of separation. Fig. 3 shows AF4 separation of Human Embryonic Kidney 293 cell homogenates obtained by gentle homogenisation (a), which was compared to the elution of the same cell homogenates obtained by tip-sonication (b), protein standards (c), and polystyrene latex particles (d), all of which were obtained under the same run conditions ($\dot{V}_{out}/\dot{V}_c$=2.0/2.5 in mL/min) [30]. Eluted components were collected into four fractions (F1–F4) for analysis with SEM and western blotting (Fig. 3e, f, respectively). Under the given run conditions, protein standards were separated by order of increasing molecular weight in normal mode, while supramicron-sized polystyrene particles were resolved by order of decreasing diameter in steric/hyperlayer mode. The two peaks (F3 and F4) shown from 5 to 15 min in Fig. 3a disappeared in Fig. 3b due to the disruption of subcellular species by sonication, and the resulting small species eluted at the first intense peak. This supports the finding that the separation of subcellular species was achieved in steric/hyperlayer mode (Fig. 3a). The intense but broad peak (F1) was presumed to be from cell wall debris, nuclei, proteins (possibly from the endoplasmic reticulum), and a few submicrometre-sized subcellular species, which were not well-resolved. However, the two distinct peaks (F3 and F4) were enriched with mitochondria and peroxisomes, respectively, through confirmation with SEM images (Fig. 3e) and western blotting using seven organelle-specific markers (3f), as well as with proteomic analysis of the two fractions using nLC-ESI-MS/MS. Fractions F1 and F2, which were poorly resolved, were collected and re-injected into AF4 under different run conditions using the normal mode of separation, and Western blot analysis of the resulting AF4 fractions confirmed the separation/enrichment of nuclei, lysosomes, and Golgi apparatuses. This study pioneered an alternate means of isolating/enriching subcellular organelles by size and shape through the careful selection of the flow rate conditions of AF4, and the collected fractions from these experiments can be utilised for additional biological experiments without deformation or denaturation due to the use of a biological buffer solution.

### 3.2. Size-dependent lipidomic analysis of exosomes

Exosomes are extracellular vesicles (30–100 nm in diameter) that are secreted by cells and are known to dispose unnecessary molecules from cells and to be involved in intercellular signalling [50,51]. Cancer cell-derived exosomes carry pathogenic proteins, enzymes, and miRNA that may influence protein production in recipient cells; consequently, they can disturb the homeostasis of recipient cells [52,53]. Because exosomes contain biomarker candidates that are differentially distributed based on exosome size, size-dependent analysis of exosomes is challenging. In an earlier report, exosomes from human neuronal stem cells were separated by FlFFF for the size-dependent proteomic analysis of exosome fractions by nLC-ESI-MS/MS [24]. FlFFF combined with MALS was utilised to determine the size distribution of exosomes from mouse melanoma cell lines, demonstrating the capability of FlFFF to perform the label-free isolation of exosomes for the purpose of characterising biologically-active components within different-sized exosomes [54]. Since exosomes carry bioactive lipids involved in immunity and inflammation, they can be utilised as biomarkers for diseases caused by lipid alteration, along with protein or miRNA biomarkers.

A recent report demonstrated a systematic investigation into the size-dependent distribution of lipids in urinary exosomes from patients with prostate cancer (PCa) compared to healthy controls using FlFFF and nUHPLC [25]. This study showed a clear difference in the sizes of urinary exosomes between PCa patients (maximum of 107.3 nm) and healthy controls (58.3 nm), as well as an increase in the exosome population of PCa patients as shown in the superimposed fractograms of Fig. 4. Western blot analysis of collected fractions revealed that fractions 2 and 3 responded to ALIX and CD9 antibodies, both of which are exosome markers, while fraction 4 did not respond to CD9. This supports the idea that exosomes or vesicles larger than ~150 nm (fraction 4) may originate from different sources of cells or organs, because CD9 is a membrane protein located at the membrane surface while ALIX is known to exist only in MVB [55]. Lipidomic analysis of exosome fractions, divided into two combined fractions (F1 and F2), showed that the lipid classes PC, PE, PEp, PS, and SM were more enriched in the smaller (<150 nm) exosome fraction (F1), whereas other classes showed no size-dependency (fold ratio plot (patient/control) in Fig. 4). General increases in PL levels may correlate with the increased expression of fatty acid synthase in cancer cells; however, the significant decreases (>2.5 fold) in neutral lipids like TAG (or TG) and DAG (or DG) in patients' exosomes may arise from the increased consumption of energy during cancer progression [56]. Statistical analysis of the alterations in individual lipid levels revealed that 11 lipid species increased and 9 lipid species

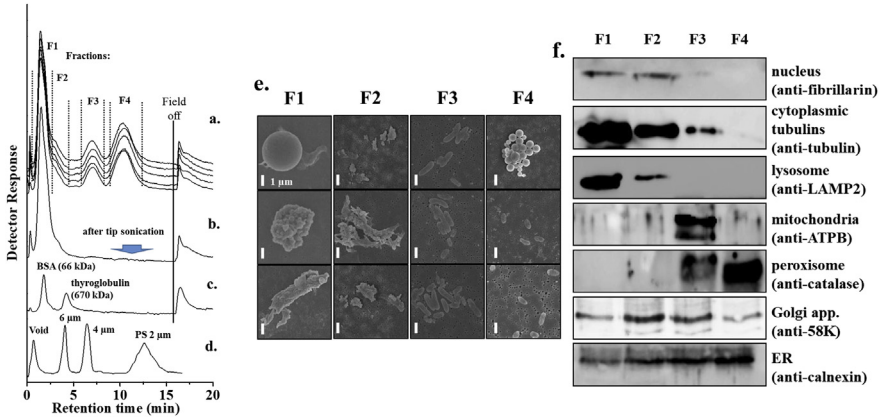


**Fig. 3.** FlFFF of (a) HEK 293T cell homogenate (5 repeated runs), cell homogenate after (b) tip-sonication, (c) BSA and thyroglobulin, and (d) PS standard mixtures. The crossflow was turned off at 17 min in a–c. All runs were obtained at $\dot{V}_{out}/\dot{V}_c$ = 2.0/2.5 mL/min (e) SEM images of 4 fractions collected during FlFFF. (f) Western blot analysis using organelle-specific antibodies. Reprinted with permission from Ref. [30]. Copyright 2015 American Chemical Society.

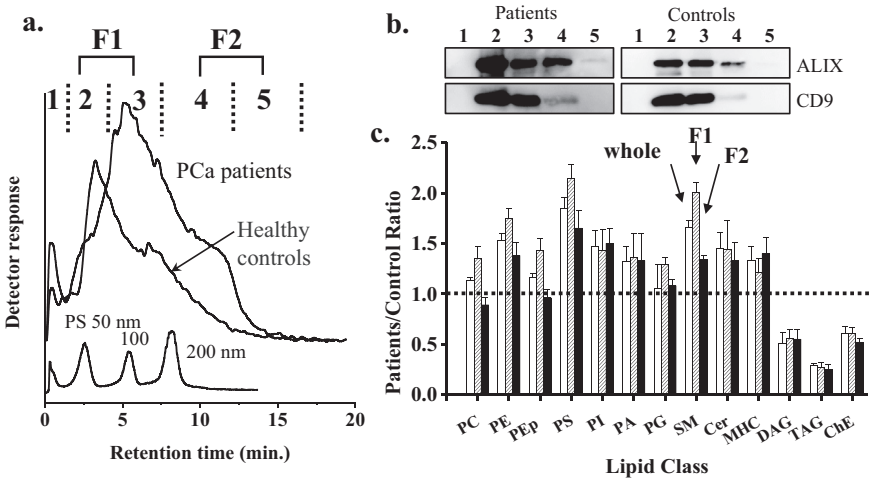


**Fig. 4.** (a) Fractograms of urinary exosomes from the pooled urine samples of four prostate cancer patients and four healthy controls, respectively. (b) Western blot results of the collected fractions. (c) Fold change ratio (patient/control) of the total lipidome by each class of lipids from non-fractionated whole exosome pellets and exosome fractions (F1 and F2). Reprinted with permission from Ref. [25]. Copyright 2017 American Chemical Society.

decreased by >2.5 fold ($p < 0.01$) in PCa patients. Among them, PG 22:6/22:6 and the two LPSs (16:0 and 18:1) were significantly increased by 7.5 and 4.5 fold, respectively, in the F1 fraction, while seven out of ten high-abundance TG species decreased more than 2.5 fold. This study demonstrated the potential of FlFFF for the high-speed separation of urinary exosomes from PCa patients, and highlighted lipidomic analysis as an alternative to prostate-specific antigens, a more common PCa marker, for the clinical diagnosis of PCa. Top-down lipidomic analysis of urinary exosomes is a promising approach for the high-speed screening of pathogenic lipids in urinary exosomes using on-line FlFFF-ESI-MS/MS.

### 3.3. *Lipidomic analysis of different lipoproteins*

Lipoproteins are globular particles that transport lipids throughout the body in blood, and are composed of neutral lipids (like hydrophobic TG and cholesteryl esters) in their core, surrounded by polar species (such as PLs) and a few proteins at their surfaces. Lipoproteins are classified as HDL, LDL, or VLDL. Since smaller and denser LDL particles (compared to VLDL), along with reduced levels of HDL, are closely associated with a higher incidence of atherosclerosis and CAD [57,58], size changes in lipoproteins and lipid alterations after disease development are of great interest. FlFFF was utilised to detect the decrease in HDL levels, the increase in LDL levels, and the size reduction of LDL particles in CAD patients' plasma compared to healthy controls [27,59]. Lipids play various roles, not only in the formation of cellular structures and energy storage, but also in signalling between cells and proteins. Since the abnormal metabolism of lipids has been known to be associated with the pathology of cardiovascular disease [60–62], molecular lipids are potentially useful signatures for clinical monitoring.

An elaborate study was designed to examine the profiles of Ox-PLs in relation to oxidation of LDL with an off-line combination of MxHF5 and nLC-ESI-MS/MS [63]. Oxidation of LDLs primarily occurs with unsaturated PLs, resulting in the formation of long-chain products, like the hydroperoxylation or hydroxylation of the unsaturated fatty acyl chain of PLs, and short-chain products, like unsaturated acyl chains truncated into shorter chains. Because Ox-PLs may stimulate the aggregation of platelets involved in the onset of cardiovascular diseases, and have a correlation with inflammatory disease [64,65], investigation of the patterns and the relative amount of Ox-PLs is important to elucidate the relationship between oxidation of LDL and cardiovascular diseases. For the semi-preparative separation of lipoproteins, an MxHF5 system composed of six or eight parallel HF5 modules (shown in the left of Fig. 5) was utilised to increase the injection volume of human plasma samples. The fractograms in the middle of Fig. 5 show the separation of a standard mixture of HDL, LDL, and VLDL (3 μg each) using a single HF module (top), compared with the separation of a plasma sample (80 μL) from a healthy control using MxHF5 (bottom). Due to the long retention of VLDL, crossflow was turned off (marked with field off) after eluting LDL in order to wash out VLDL. Standard lipoproteins were detected at 280 nm, but plasma lipoproteins were detected at 600 nm after staining with Sudan Black B, demonstrating the ability of both a single HF5 channel and MxHF5 to separate different lipoproteins [63]. HDL, LDL, and VLDL fractions were collected from pooled plasma samples from the CAD patient group and healthy controls (without staining) using MxHF5. Then, lipids from each lipoprotein fraction were extracted and analysed by nanoflow liquid chromatography-electrospray ionisation-tandem mass spectrometry (nLC-ESI-MS/MS). Structural determination of lipid molecules by data-dependent CID experiments yielded the identification of a total of 283 PLs (including 123 Ox-PLs) from controls, and 315 PLs (including 169 Ox-PLs) from patients, supporting the hypothesis that oxidation of PLs is significantly higher in CAD patients. It was discovered that single hydroxylation was most prevalent among the identified forms of Ox-PLs, including hydroperoxylation or short-chain products. Moreover, hydroxylation of PLs occurred primarily in PLs containing a saturated acyl chain (16:0 and 18:0) in the sn-1 position of the glycerol backbone of PL, along with a polyunsaturated acyl chain (>2 double bonds) at sn-2, as shown in the right side of Fig. 5. The degree of hydroxylation of these PL species ranged from 10 to 30% in CAD patients compared to healthy controls.

Quantitative lipidomic comparison of lipoproteins was accomplished using plasma samples from patients with ACS and stable CAD. ACS can occur during the course of CAD when atherosclerotic plaques in the coronary arterial wall suddenly rupture and impede blood circulation, leading to unstable angina, myocardial infarction, and sudden cardiac death. Individual plasma samples from patients – 10 with ACS (age = 55.2 ± 5.5) and 10 with stable CAD (age = 57.3 ± 6.9) – were separated using a semi-preparative AF4 channel (initial and final channel widths of 4.4 and 0.4 cm,

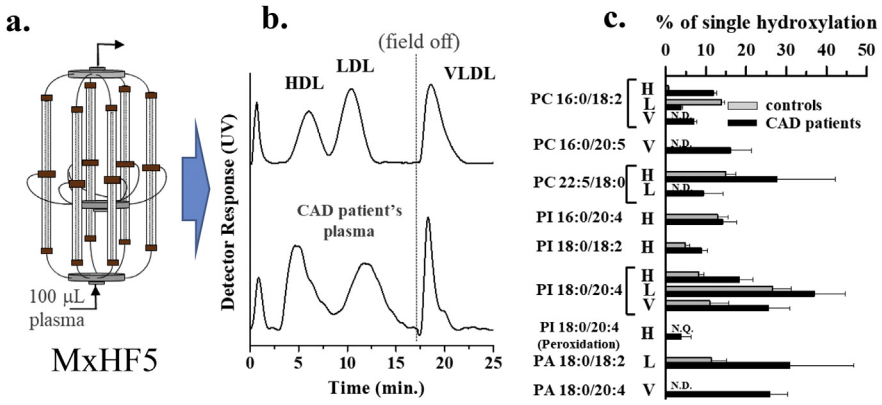


**Fig. 5.** (a) Schematic of the MxHF5 channel. Fractograms of (b) a standard mixture of HDL, LDL, and VLDL, and a human plasma sample with CAD (SBB-stained). (c) Percentage of singly-hydroxylated species compared to the original intact molecule for selected Ox-PL species, quantified from control and patient samples. H, L, and V represent HDL, LDL, and VLDL fractions, respectively. N.D. = not detected, and N.Q. = not quantifiable. Reprinted with permission from Ref. [63]. Copyright 2015 American Chemical Society.

respectively) [66]. Lipids that were extracted from the HDL and LDL fractions of each patient sample were analysed with two-stage nano-flow ultra high-performance liquid chromatography (nUHPLC)-ESI-MS/MS experiments for non-targeted lipid identification, with CID experiments followed by targeted quantification using the selected reaction monitoring (SRM) method. A total of 365 lipids from 13 lipid classes – including ceramides (Cer), SM, PEp, DG, and TG – were quantified. Among these lipids, two high-abundance LPC species (16:0 and 18:0) were found to be significantly increased ($p < 0.05$) by > 2-fold in ACS patients in the HDL fraction, and (18:0, 22:6)-DG was increased by 3.5-fold in the LDL fraction. Most high-abundance TG species decreased by > 2-fold in both the HDL and LDL fractions. Related studies showed that LPCs with saturated or monounsaturated acyl chains increased inflammation and atherosclerosis [67], and its level was elevated in patients with ACS, and to a larger degree in patients with non-ST-elevation myocardial infarction [68]. However, lipoprotein-specific lipidomic analysis with FlFFF and nLC-ESI-MS/MS revealed that the relative increase of LPC levels in ACS patients occurs primarily in the HDL fraction, confirming the strong correlation between ACS and HDLs.

In a recent report, a similar approach was used to identify the lipoprotein-specific lipid alterations in patients with AD and MCI [69]. AD is an irreversible neurodegenerative disorder consisting of progressive memory loss distinguished by the accumulation of neuritic plaques enriched with amyloid β and hyperphosphorylated tau proteins in the brain; MCI is a transitional state between normal ageing-related cognitive changes and AD [70–72]. Because 80% of MCI is known to progress to AD within 6 years [73], detection of this early stage of disease is a challenging task. The development of molecular markers from common biological fluids rather than from cerebrospinal fluid (CSF) is preferable, as obtaining CSF is rather invasive and risky. Using semi-preparative scale AF4, fractions of HDL and a combined LDL/VLDL were isolated from individual plasma samples from the following groups: 14 AD patients (age = 72.6 ± 3.1), 23 MCI patients (age = 72.5 ± 3.1), and 13 individuals with normal cognition (age = 71.5 ± 3.6). Quantitative analysis of 363 lipids by nUHPLC-ESI-MS/MS showed that the total level of most lipid classes increased more than 2-fold in the LDL/VLDL fraction of AD patients, while the levels of DG and PG decreased in the HDL fraction, as shown with three lipid classes (DG, TG, and PE; Fig. 6a). Corrected peak area represents the peak area of individual lipid species relative to that of an internal standard (1 pmol) specific to each lipid class. Statistical evaluation of the quantified results showed that 14 high-abundance lipids – including PE, Cer, PA, PI, DG, and TG – were significantly altered (>2-fold, $p < 0.01$) in the LDL/VLDL fraction of AD patient samples, with increases in the HDL fraction of 2 PEs (34:2 and 36:2) and TG (50:1). Among them, the three lipids (TG 50:1, DG 18:1_18:1, and PE 36:2) in the LDL/VLDL fractions of AD patients showed a strong correlation (2–4 fold increases) with increases in the degree of brain damage, measured from structural brain magnetic resonance imaging, a hallmark of AD pathology regardless of diagnosis (Fig. 6b). This rating increases with the severity of brain damage, classified into periventricular white matter lesions (PVWML), deep white matter lesions (DWML), and medial temporal lobe atrophy in the left (LMTA) and right (RMTA) brain. When receiver operating characteristic analysis was carried out for the lipid changes in the three species from the MCI group, in combination with scores from the MMSE, a common test for cognitive impairment, the area under curve (AUC) values increased to 0.833–0.917, suggesting that the reliability of clinical diagnosis of MCI can be improved. This also supported the possibility that plasma lipids can be utilised to facilitate mass screenings for dementia-risk by combining simple MMSE and lipidomic analysis of blood, rather than relying on cerebrospinal fluid measurement or neuroimaging, both of which are expensive.

## 4. On-line hyphenation of FlFFF with MS

Proteomic and lipidomic analysis often require a high-performance separation/isolation of biological complexes, which is a critical step to simplify or purify target materials from a complex mixture prior to MS analysis. A great number of proteomic and lipidomic applications are being carried out to find out the pathological roles of proteins and lipids in the development of diseases, and to develop biomarkers for diseases. However, even after the isolation/purification steps, the bottom-up approach of proteomic and lipidomic analysis requires complicated enzymatic digestion and lipid extraction, respectively, prior to LC-ESI-MS/MS, although it does provide excellent identification and quantification results. A top-down approach can bypass the sample preparation procedures with the advantage of obtaining precise information on protein isoforms or post-translational modifications of proteins. However, current available methods for intact protein separation are mostly based on liquid chromatography with the use of organic solvents, which may induce dissociation of protein subunits or denaturation as well as unwanted interactions with the stationary phase.

FlFFF can be directly hyphenated with MS for top-down proteomic or lipidomic analysis, which is a powerful alternative method for the high-speed screening of target proteins or lipids (Fig. 2b). Moreover, ICP-MS can be connected on-line with FlFFF for

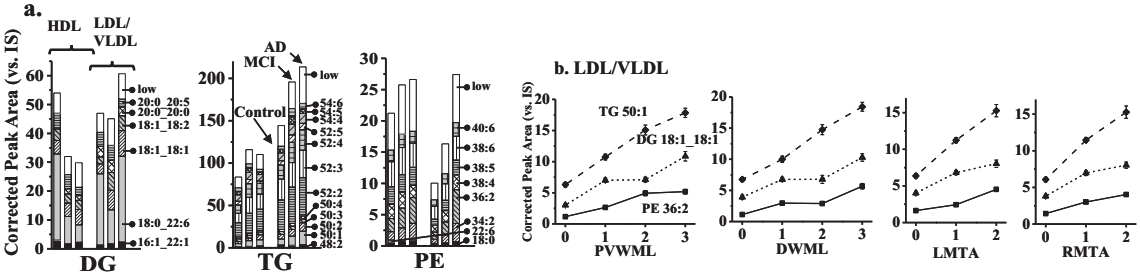


**Fig. 6.** (a) Stacked bar graphs of individual lipid molecules in three lipid classes (based on the summation of corrected peak area) in the HDL and LDL/VLDL fractions of control, MCI, and AD groups. The "low" represents the summed amount of remaining low-abundance species. (b) Correlation of the three prominent lipid species (TG 50:1, DG 18:1_18:1, and PE 36:2) in LDL/VLDL to the ratings of hyperintensity of deep white matter lesion (DWML), periventricular white matter lesion (PVWML), left medial temporal lobe atrophy (LMTA), and right medial temporal lobe atrophy (RMTA), as measured by structural MRI. Reprinted with permission from Ref. [69]. Copyright 2018 Elsevier B.V.

the analysis of metals and their distributions in metalloproteins in blood. Due to the use of an unobstructed channel space for protein separation in biocompatible buffer solutions, FlFFF is suitable for handling biomaterials in their intact conditions and provides simultaneous desalting during separation. The latter is a great asset for utilising on-line FlFFF with MS, since the salts contained in most biological samples strongly interfere with direct MS analysis. A difficulty in the on-line analysis of a conventional FlFFF system and MS arises from the relatively high flow rate of FlFFF, typically at least a few hundred μL/min. This can be overcome by reducing the channel dimensions to assemble a mAF4 which can be operated at 10–20 μL/min in a 7 cm long channel with an initial and a final breadth of 0.7 and 0.3 cm, respectively [74]. Fig. 7a demonstrates the ability of mAF4-ESI-MS/MS to separate carbonic anhydrase (CA, 29 kDa, 0.5 μg), transferrin (78 kDa, 1.0 μg), and the dimeric form of transferrin, for which the fractogram was represented with a base peak MS signal. The outflow rate (12 μL/min) of mAF4 was split such that one-third (4 μL/min) was fed into ESI-MS in this run. Fig. 7b shows the MS spectrum of multiply-charged ions of transferrin at the time interval 9.6–9.9 min, yielding a molar mass of 78,008 Da. The baseline noise was much cleaner than the MS spectra from direct infusion of transferrin without mAF4 (not shown here). Data-dependent CID experiments on $[M+45H]^{+45}$ yielded the possibility of identifying amino acid sequences. Another interesting feature was the detection of transferrin dimers by MS spectra: the characteristic highly-charged ion peaks of dimer molecules (i.e. +75 ions) are shown at a relatively weak intensity between two nearby ion peaks, of which each individual peak was presumed to be the overlap of two differently-charged ions, e.g. +38 for monomers and +76 for dimers, and +37 for monomers and +74 for dimers (Fig. 7c). Deconvolution of spectra indicated the presence of a dimer peak at *m*/*z* 156,294 Da, supporting the conclusion that some dimers were dissociated into monomers during ESI, but multimeric aggregates can still be characterised by mAF4-ESI-MS/MS. This study also demonstrated the flexibility of mAF4-ESI-MS/MS. Proteins or biological samples can be directly injected into mAF4-ESI-MS/MS without preliminary desalting or solvent exchange because small molecules or salts in the sample solution are readily filtered out during mAF4 operation.

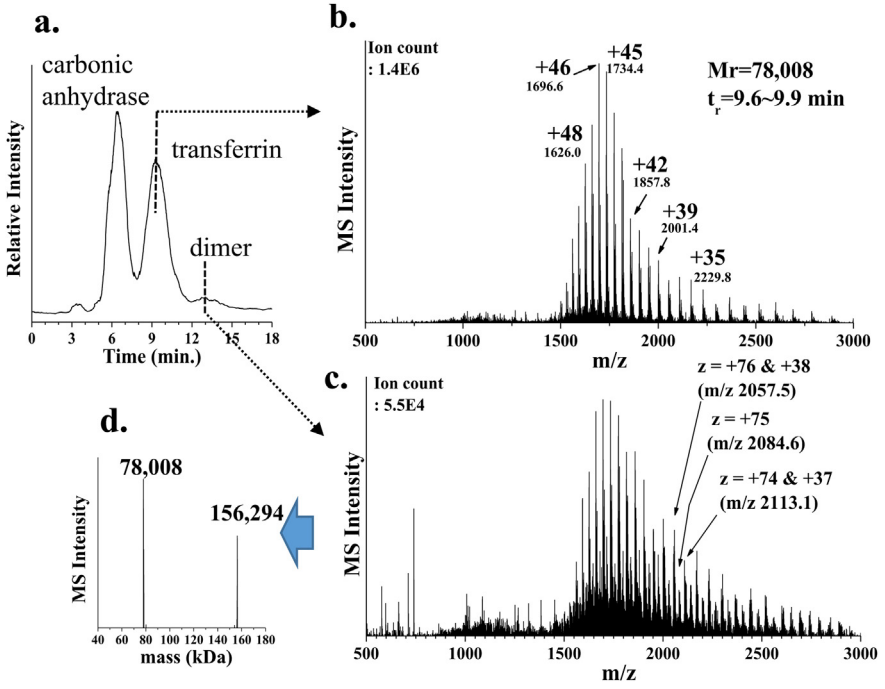


**Fig. 7.** (a) Base peak fractogram (BPF) of AF4-ESI-MS for the separation of CA and transferrin obtained at _V out/_V c = 0.012/0.49 mL/min. Full scan MS spectra for (b) transferrin and (c) transferrin dimer showing mixed ion spectrum of multiply-charged monomers and dimers. (d) The deconvoluted MS spectrum showing the transferrin monomer and dimer. Reprinted with permission from Ref. [74]. Copyright 2011 American Chemical Society.

### 4.1. Top-down lipidomic analysis of lipoproteins

The off-line combination of FlFFF and LC-ESI-MS/MS for lipid analysis of lipoproteins provides comprehensive qualitative and quantitative information on lipids in different lipoproteins, which can then be utilised to develop lipid biomarkers for disease diagnosis and risk assessment. This offers a high throughput, highly sensitive analysis of lipids in different lipoproteins. However, off-line analysis requires a separate lipid extraction process to collect lipoprotein fractions prior to LC-ESI-MS/MS analysis. By utilising the mAF4-ESI-MS/MS platform, lipoprotein particles eluted from mAF4 can be injected to MS for the direct analysis of lipids without extraction once the channel outflow rate is properly adjusted for ESI. A top-down lipidomic analysis using mAF4-ESI-MS/MS can provide the high-speed screening of lipid molecules once target lipid species are established. Moreover, on-line desalting can be advantageous in mFlFFF-ESI-MS/MS, which enhances the direct ionisation of lipids in lipoproteins [75].

The possibility of on-line lipid identification was successfully demonstrated with 52 lipid species in HDL and LDL from patients with CAD, along with the SRM-based quantification of ApoA1 [75], a major diagnostic protein marker exclusively found in HDL, to assess cardiovascular diseases involved in cholesterol homeostasis. This study showed the ability of mAF4-ESI-MS/MS to selectively quantify both lipids and ApoA1 without isolating ApoA1 from plasma proteins. An additional study successfully developed a suitable SRM-based lipid quantification method by adding a small protein, carbonic anhydrase (CA, 29 kDa), to plasma samples as an internal standard. This method is utilised to detect the SRM transition of a multiply-charged protein ion ($m/z$ 1613 for $[M+18H]^{+18}$) into a high-abundance peptide fragment ion ($m/z$ 1512 for $y_{67}^{+5}$) [76]. This bypasses the uncertainty in lipid quantification that usually occurs when external lipid standards are added to a plasma sample, because the added lipids are not retained in the FlFFF channel due to their small size and cannot be evenly absorbed by lipoproteins of different sizes. Fig. 8a shows the MS fractograms of HDL and LDL from human blood plasma samples (2.5 μL injected, 5 repeated runs) based on the MS detection of PC 36:4, which was obtained by the relative peak intensity of the SRM quantifier ion $m/z$ 599.6 ($[M + H\text{-}183]^+$). The latter is a characteristic product ion produced by a cleavage of the phosphocholine head group (183 Da) from the SRM transition of the precursor ion $m/z$ 782.6 ($[M+H]^+$), to that of an internal standard (CA, 0.2 μg) [76]. A CID experiment for PC 36:4 during 3.6–3.9 min of the mAF4-ESI-MS/MS run yielded a clear MS/MS spectrum (Fig. 8b), showing the typical fragment ions formed by the loss of the acyl chain in the form of ketene at $m/z$ 544.5 and 496.4, and carboxylic acid at $m/z$ 526.6 and 478.4, with the differentiation of the acyl chains location at $R_1$ and $R_2$, respectively. SRM quantification of targeted lipid species from the HDL and LDL fractions of CAD patient plasma (n = 10) showed significant decreases (>2.5 fold, $p < 0.01$) in 5 PLs of HDL, but significant increases in 10 lipid species of LDL (aside from the two PE species), in comparison to healthy controls (n = 10). While lipoproteins in CAD patients showed a decrease in HDL level and an increase in LDL level with a substantial decrease in LDL sizes, not all lipid species followed the same trend. For example, PE 38:4 in Fig. 8c showed a decrease in its level in the LDL fractions of patients, which was opposite to what was observed for most lipid species quantified in this study. It also showed a decrease in the retention time of LDL, which supports ideas regarding the reduction of LDL sizes upon the development of CAD.

This study demonstrated that top-down lipidomic analysis using mAF4-ESI-MS/MS is promising for quantitatively monitoring the alterations in lipid levels in HDL and LDL without the separate isolation of lipoproteins followed by lipid extraction for LC-ESI-MS/MS analysis. By adding carbonic anhydrase to plasma samples as an internal standard, SRM quantification of individual PL levels in both HDL and LDL can be achieved without the difficulty of homogenising lipid standards over differently-sized lipoprotein particles in plasma samples. Moreover, direct lipid analysis offers the bonus of eliminating organic solvent extraction, reducing the possible loss of lipids during preparation and also reducing total analysis time. A weakness of this approach is an ion suppression effect for low-abundance lipid species due to the simultaneous ionisation of all lipid species in lipoprotein particles; however, a thorough study incorporating high resolution MS is needed to evaluate the effect of this ion suppression. Nonetheless, mAF4-ESI-MS/MS can be a powerful screening method for abundant lipids for therapeutic intervention studies of lipoprotein lipids related to cardiovascular disorders.

### 4.2. Direct analysis of metals in metalloproteins by mAF4-ICPMS

Metalloproteins are metal-binding proteins, and approximately one-third of all proteins in nature contain metals, which play important functions in signal transduction, respiration, and the transportation of proteins [77]. Although metal concentrations in metalloproteins are very low, imbalances in essential metals may cause a change in the structure and function of these proteins, leading to the onset of diseases such as Alzheimer's disease (Cu, Fe, and Zn) [78], Wilson and Menkes diseases (Cu) [79], and atherosclerosis (Cu and Fe) [80]. Analysis of metals in metalloproteins has

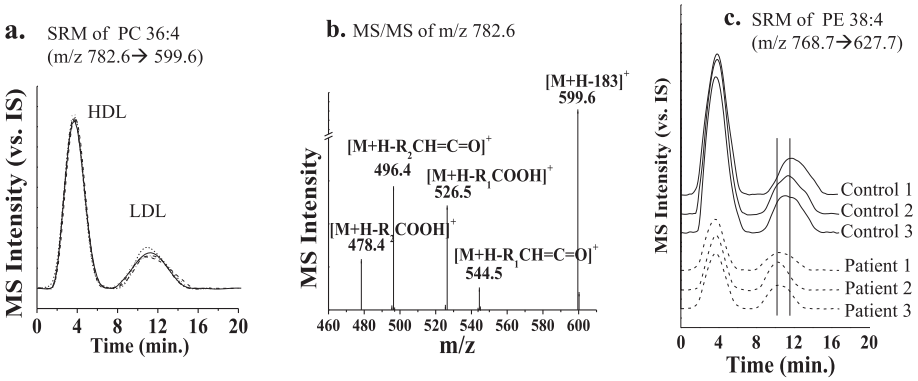


**Fig. 8.** (a) SRM monitoring (5 repeated runs) of PC 36:4 during mAF4-ESI-MS/MS of a healthy human plasma sample. (b) MS/MS spectra of the precursor ion $m/z$ 782.6 at 3.6–3.9 min, showing characteristic fragment ion spectra of PC 36:4. (c) Comparison of SRM fractograms based on PE 38:4 ($m/z$ 768.7 → 627.7) from three controls and three patient samples. Reprinted with permission from Ref. [76]. Copyright 2014 Elsevier B.V.

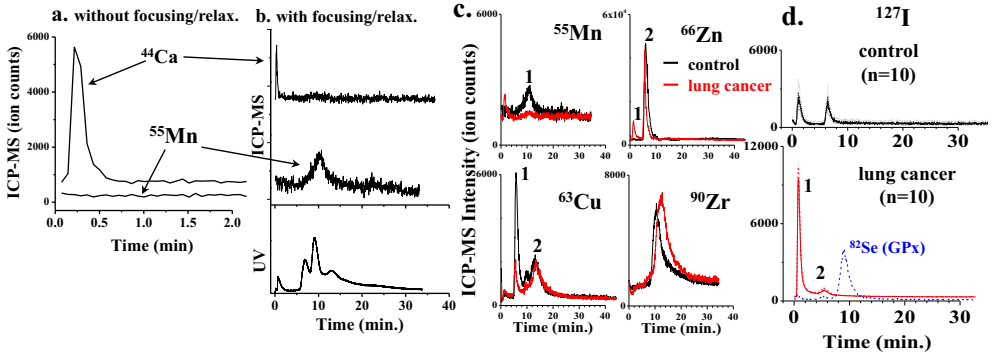


**Fig. 9.** Comparison of element detection (44Ca and 55Mn) for a healthy normal plasma sample (depleted) (a) without focusing/relaxation (direct passage of plasma through mAF4 channel to ICPMS) and (b) with focusing/relaxation for size separation of plasma proteins by mAF4-ICPMS and mAF4-UV detection. (c) Elemental fractograms of $^{55}$Mn, $^{63}$Cu, $^{66}$Zn, and $^{90}$Zr from metalloproteins of pooled healthy normal plasma as a control (n = 10, black) and pooled plasma from patients with lung cancer (n = 10, red) (after depletion) by mAF4-ICPMS. (d) Comparison of individual peaks of $^{127}$I between 10 controls and 10 patients. This was superimposed with the MS signal for $^{82}$Se from GPx as an internal standard. Reprinted with permission from Ref. [81]. Copyright 2016 American Chemical Society.

been carried out through chromatographic methods (RPLC or HILIC) combined with ICPMS, which provide highly sensitive metal detection. Due to the passage of metalloproteins through packing materials in organic solvents, the possible deformation of protein conformation and unwanted interactions with stationary phases may induce a dissociation of metals from the metal-protein complex. As an alternative to LC-ICPMS, FlFFF can be on-line coupled with ICP-MS for size separation of proteins followed by direct detection of metals associated with metalloproteins. With mAF4-ICPMS, the outflow rates are easily maintained at a few μL/min, which can be directly fed to ICPMS without splitting as shown in the lower right of Fig. 2.

The application of this technique resulted in the successful analysis of metals in metalloproteins from plasma proteome samples from patients with lung cancer in comparison to healthy controls (Fig. 9) [81]. Outstanding features of mAF4-ICPMS for metal analysis of plasma samples include the simultaneous removal of free metal ions that are not bound to metalloproteins, because free metals can be washed out via crossflow during the focusing/relaxation stage prior to an AF4 operation, and the enrichment effect on low-abundance proteins. Fig. 9a, b shows the differences in metal ion detection from plasma samples with or without the focusing/relaxation procedure. The injection volume of the plasma sample was 20 μL of the depleted sample (diluted during the depletion of albumin and IgG from a raw plasma sample), equivalent to 4 μL of raw plasma from a healthy normal adult. In the breakthrough run (Figure 9a), $^{44}$Ca was detected with an intense signal but $^{55}$Mn was not at all detected due to skipping the focusing/relaxation step. However, the $^{44}$Ca peak mostly disappeared after focusing/relaxation with the appearance of the $^{55}$Mn peak at around 10 min (Fig. 9b), implying that free/unbound $^{44}$Ca ions were washed through the channel membrane and Mn-containing metalloproteins were enriched and retained in mAF4. Fig. 9c, d shows mAF4-ICPMS fractograms for $^{55}$Mn, $^{63}$Cu, $^{66}$Zn, and $^{90}$Zr, comparing a pooled healthy control (black) to a pooled lung cancer (red) plasma sample (n = 10 for both), along with the superimposed fractograms (9d) for $^{127}$I from the individual samples of 10 patients and 10 controls. The $^{82}$Se peak in Fig. 9d was from an internal standard, glutathione peroxidase (GPx, 84 kDa), which was added to plasma samples. $^{55}$Mn and the first peak of $^{63}$Cu showed significant decreases in intensities in patient plasma, while peak 1 of both $^{66}$Zn and $^{127}$I showed discrete increases, which represent the dissociation of protein complexes into smaller subunits.

Furthermore, changes in the retention times of metalloproteins may imply changes in size or molar mass through the formation of complexes or the dissociation of subunits. From quantitative comparison of the peak area of patients to controls (P/C) for the 12 elements examined, seven elements ($^{55}$Mn, $^{60}$Ni, $^{63}$Cu, $^{66}$Zn, $^{90}$Zr, $^{127}$I, and $^{137}$Ba) showed significant changes ($p < 0.01$) in cancer patients. Protein fractions were collected during mAF4 separation for the quantitative comparison of metalloproteins in lung cancer by nLC-ESI-MS/MS using isotope-coded carbanidomethylation method. The relative quantification (P/C) of some metalloproteins associated with $^{55}$Mn, $^{60}$Ni, $^{63}$Cu, and $^{66}$Zn showed similar patterns of increases or decreases in their levels as observed with the corresponding metal levels obtained by mAF4-ICPMS.

This pioneering work suggests that, once metalloprotein biomarkers have been established, online hyphenation of mAF4 and ICPMS can be utilised as a high-speed metal screening method for metalloproteins whose levels are altered during disease development. Usage of mAF4-ICPMS provides a few advantages for the direct analysis of metals in metalloproteins, such as minimal disruption of metal-protein complex structures due to the use of an aqueous buffer solution, enrichment of low-abundance metalloproteins during the focusing/relaxation procedure, and the ability to distinguish metals in metalloproteins from free unbound metals due to the removal of free metal ions and salts in biological samples for ICPMS analysis without a separate desalting step.

## 5. Conclusion

The primary advantages of utilising FlFFF for the separation of biological macromolecules are the biocompatibility of the carrier liquid, which is the same as the aqueous buffer solution in which samples are dispersed, and the soft nature of separation based on flow dynamics without the need for interactions of sample materials with stationary phase or gel media. Due to these characteristics, biomaterials can maintain their intact properties after fractionation, and the collected fractions can be used to identify biologically active components or to investigate the size-dependent profiles of proteomes or metabolomes, including lipidomes, with several available methods. A bottleneck for the secondary analysis of collected fractions is the limited injection amount for most FlFFF channels, including AF4, FI-AF4, and HF5. Typical injection amounts of analytical-scale FlFFF are less than tens of microliters of plasma, about 100 μL of cell lysates (from ~2.5 × $10^5$ cells in 4 mL), and a few μg of lipoprotein standards. These amounts can be increased by several folds when semi-preparative scale FlFFF channels are utilised, but it is still desirable to develop a preparative-scale FlFFF channel with the proper channel design and appropriate flow

optimisations. Expanding the breadth of a rectangular FlFFF channel can increase the throughput of FlFFF channels; however, the difficulty lies in the construction of a wide, flat channel from a single piece. MxHF5, which consists of dozens of HF modules, is a good alternative to increase throughput providing that the same pressure is maintained in each individual HF5 module.

On-line hyphenation of FlFFF with MS has great potential for biological applications because it combines the separation and comprehensive characterisation of bioactive components contained in large molecular complexes. Since direct FlFFF-MS analysis bypasses sample preparation procedures, it boosts the speed of analysis with minimal sample-loss during preparation. Moreover, on-line desalting during FlFFF separation offers a great advantage for the direct analysis of intact molecules without the loss of conformation through the use of organic solvents or surfactants, as is the case in chromatographic or gel-based methods. FlFFF-MS can be integrated into a high-speed screening method to differentiate protein levels in biological fluids, lipids in exosomes or lipoproteins, metals in metalloproteins, and possibly miRNAs and other pathogenic molecules associated with large complexes that are involved in the progression of diseases or during drug intervention. For on-line FlFFF-MS, technical advances are necessary to develop a microscale FlFFF channel for the direct coupling with MS and enhancement of separation resolution.

## Acknowledgements

This study was supported by grant NRF-2018R1A2A1A05019794 from the National Research Foundation (NRF) of Korea.

## References

[1] C.P. Satori, V. Kostal, E.A. Arriaga, Anal. Chim. Acta 753 (2012) 8.
[2] N.R. Sims, M.F. Anderson, Nat. Protoc. 3 (2008) 1228.
[3] H.T. Hornig-Do, G. Gunther, M. Bust, P. Lehnartz, A. Bosio, R.J. Wiesner, Anal. Biochem. 389 (2009) 1.
[4] L.A. Herzenberg, D. Parks, B. Sahaf, O. Perez, M. Roederer, L.A. Herzenberg, Clin. Chem. 48 (2002) 1819.
[5] B.A. Griffin, M.J. Caslake, B. Yip, G.W. Tait, C.J. Packard, J. Shepherd, Atherosclerosis 83 (1990) 59.
[6] J. Schiller, O. Zschornig, M. Petkovic, M. Muller, J. Arnhold, K. Arnold, J. Lipid Res. 42 (2001) 1501.
[7] H.Y. Sun, S.F. Chen, M.D. Lai, T.T. Chang, T.L. Chen, P.Y. Li, D.B. Shieh, K.C. Young, Clin. Chim. Acta 411 (2010) 336.
[8] S.B. Alabakovska, B.B. Todorova, D.D. Labudovic, K.N. Tosheska, Clin. Chim. Acta 317 (2002) 119.
[9] R.M. Krauss, D.J. Burke, J. Lipid Res. 23 (1982) 97.
[10] P. Wiesner, K. Leidl, A. Boettcher, G. Schmitz, G. Liebisch, J. Lipid Res. 50 (2009) 574.
[11] J.C. Giddings, Anal. Chem. 53 (1981) 1170.
[12] J.C. Giddings, Science 260 (1993) 1456.
[13] P. Reschiglian, M.H. Moon, J. Proteomics 71 (2008) 265.
[14] S.K. Williams, J.R. Runyon, A.A. Ashames, Anal. Chem. 83 (2011) 634.
[15] K.G. Wahlund, J. Chromatogr. A 1287 (2013) 97.
[16] S.K. Ratanathanawongs, J.C. Giddings, Anal. Chem. 64 (1992) 6.
[17] D. Kang, M.H. Moon, Anal. Chem. 78 (2006) 5789.
[18] K.H. Kim, M.H. Moon, Anal. Chem. 81 (2009) 1715.
[19] A. Hawe, S. Romeijn, V. Filipe, W. Jiskoot, J. Pharm. Sci. 101 (2012) 4129.
[20] P. Reschiglian, B. Roda, A. Zattoni, M. Tanase, V. Marassi, S. Serani, Anal. Bioanal. Chem. 406 (2014) 1619.
[21] J. Ashby, K. Flack, L.A. Jimenez, Y.K. Duan, A.K. Khatib, G. Somlo, S.E. Wang, X.P. Cui, W.W. Zhong, Anal. Chem. 86 (2014) 9343.
[22] K. Flack, L.A. Jimenez, W. Zhong, Methods Mol. Biol. 1509 (2017) 161.
[23] J. Ashby, S. Schachermeyer, Y. Duan, L.A. Jimenez, W. Zhong, J. Chromatogr. A 1358 (2014) 217.
[24] D. Kang, S. Oh, S.M. Ahn, B.H. Lee, M.H. Moon, J. Proteome Res. 7 (2008) 3475.
[25] J.S. Yang, J.C. Lee, S.K. Byeon, K.H. Rha, M.H. Moon, Anal. Chem. 89 (2017) 2488.
[26] H. Zhang, D. Freitas, H.S. Kim, K. Fabijanic, Z. Li, H. Chen, M.T. Mark, H. Molina, A.B. Martin, L. Bojmar, J. Fang, S. Rampersaud, A. Hoshino, I. Matei, C.M. Kenific, M. Nakajima, A.P. Mutvei, P. Sansone, W. Buehring, H. Wang, J.P. Jimenez, L. Cohen-Gould, N. Paknejad, M. Brendel, K. Manova-Todorova, A. Magalhaes, J.A. Ferreira, H. Osorio, A.M. Silva, A. Massey, J.R. Cubillos-Ruiz, G. Galletti, P. Giannakakou, A.M. Cuervo, J. Blenis, R. Schwartz, M.S. Brady, H. Peinado, J. Bromberg, H. Matsui, C.A. Reis, D. Lyden, Nat. Cell Biol. 20 (2018) 332.
[27] I. Park, K.J. Paeng, Y. Yoon, J.H. Song, M.H. Moon, J. Chromatogr. B Analyt. Technol. Biomed Life Sci. 780 (2002) 415.
[28] J.Y. Lee, H.K. Min, D. Choi, M.H. Moon, J. Chromatogr. A 1217 (2010) 1660.
[29] D. Kang, S. Oh, P. Reschiglian, M.H. Moon, Analyst 133 (2008) 505.
[30] J.S. Yang, J.Y. Lee, M.H. Moon, Anal. Chem. 87 (2015) 6342.
[31] H. Lee, S.K. Williams, K.L. Wahl, N.B. Valentine, Anal. Chem. 75 (2003) 2746.
[32] P. Reschiglian, A. Zattoni, B. Roda, L. Cinque, D. Melucci, B.R. Min, M.H. Moon, J. Chromatogr. A 985 (2003) 519.
[33] A. Citkowicz, H. Petry, R.N. Harkins, O. Ast, L. Cashion, C. Goldmann, P. Bringmann, K. Plummer, B.R. Larsen, Anal. Biochem. 376 (2008) 163.
[34] Y. Chen, Y. Zhang, Y.F. Zhou, J. Luo, Z.G. Su, Vaccine 34 (2016) 3164.
[35] J.C. Giddings, F.J. Yang, M.N. Myers, Science 193 (1976) 1244.
[36] K.G. Wahlund, J.C. Giddings, Anal. Chem. 59 (1987) 1332.
[37] K.G. Wahlund, J. Chromatogr. A 1218 (2011) 6848.
[38] M.H. Moon, H. Kwon, I. Park, Anal. Chem. 69 (1997) 1436.
[39] M.H. Moon, P.S. Williams, H. Kwon, Anal. Chem. 71 (1999) 2657.
[40] M.H. Moon, I. Hwang, J. Liq. Chromatogr. Relat. Technol. 24 (2001) 3069.
[41] B. Kim, S. Woo, Y.S. Park, E. Hwang, M.H. Moon, Anal. Bioanal. Chem. 407 (2015) 1327.
[42] S. Woo, J.Y. Lee, W. Choi, M.H. Moon, J. Chromatogr. A 1429 (2016) 304.
[43] W.J. Lee, B.R. Min, M.H. Moon, Anal. Chem. 71 (1999) 3446.
[44] D. Kang, M.H. Moon, Anal. Chem. 77 (2005) 4207.
[45] J.Y. Lee, K.H. Kim, M.H. Moon, J. Chromatogr. A 1216 (2009) 6539.
[46] B.N. Barman, E.R. Ashwood, J.C. Giddings, Anal. Biochem. 212 (1993) 35.
[47] D.C. Chan, Cell 125 (2006) 1241.
[48] L.A. Huber, K. Pfaller, I. Vietor, Circ. Res. 92 (2003) 962.
[49] P.H. Reddy, M.F. Beal, Brain Res. Brain Res. Rev. 49 (2005) 618.
[50] K. Denzer, M.J. Kleijmeer, H.F.G. Heijnen, W. Stoorvogel, H.J. Geuze, J. Cell Sci. 113 (2000) 3365.
[51] G. Raposo, W. Stoorvogel, J. Cell Biol. 200 (2013) 373.
[52] G. Muller, C. Jung, J. Straub, S. Wied, W. Kramer, Cell. Signal. 21 (2009) 324.
[53] G. Muller, M. Schneider, G. Biemer-Daub, S. Wied, Cell. Signal. 23 (2011) 1207.
[54] K.E. Petersen, E. Manangon, J.L. Hood, S.A. Wickline, D.P. Fernandez, W.P. Johnson, B.K. Gale, Anal. Bioanal. Chem. 406 (2014) 7855.
[55] M.P. Oksvold, A. Kullmann, L. Forfang, B. Kierulf, M. Li, A. Brech, A.V. Vlassov, E.B. Smeland, A. Neurauter, K.W. Pedersen, Clin. Ther. 36 (2014) 847.
[56] J. Suburu, Y.Q. Chen, Prostag. Other Lipid Mediat. 98 (2012) 1.
[57] M. Navab, S.Y. Hama, S.T. Reddy, C.J. Ng, B.J. Van Lenten, H. Laks, A.M. Fogelman, Curr. Opin. Lipidol. 13 (2002) 363.
[58] I. Rajman, M.J. Kendall, R. Cramb, R.L. Holder, M. Salih, M.D. Gammage, Atherosclerosis 125 (1996) 231.
[59] M. Rambaldi, M. Baranzoni, P. Coppolecchia, J.N. Moschello, F. Novaco, Clin. Chem. Lab. Med. 45 (2007) 774.
[60] J.M. Cheng, M. Suoniemi, I. Kardys, T. Vihervaara, S.P. de Boer, K.M. Akkerhuis, M. Sysi-Aho, K. Ekroos, H.M. Garcia-Garcia, R.M. Oemrawsingh, E. Regar, W. Koenig, P.W. Serruys, R.J. van Geuns, E. Boersma, R. Laaksonen, Atherosclerosis 243 (2015) 560.
[61] Z.H. Alshehry, P.A. Mundra, C.K. Barlow, N.A. Mellett, G. Wong, M.J. McConville, J. Simes, A.M. Tonkin, D.R. Sullivan, E.H. Barnes, P.J. Nestel, B.A. Kingwell, M. Marre, B. Neal, N.R. Poulter, A. Rodgers, B. Williams, S. Zoungas, G.S. Hillis, J. Chalmers, M. Woodward, P.J. Meikle, Circulation 134 (2016) 1637.
[62] C. Syme, S. Czajkowski, J. Shin, M. Abrahamowicz, G. Leonard, M. Perron, L. Richer, S. Veillette, D. Gaudet, L. Strug, Y. Wang, H. Xu, G. Taylor, T. Paus, S. Bennett, Z. Pausova, Circulation 134 (2016) 1629.
[63] J.Y. Lee, S.K. Byeon, M.H. Moon, Anal. Chem. 87 (2015) 1266.
[64] S. Ehara, M. Ueda, T. Naruko, K. Haze, A. Itoh, M. Otsuka, R. Komatsu, T. Matsuo, H. Itabe, T. Takano, Y. Tsukamoto, M. Yoshiyama, K. Takeuchi, J. Yoshikawa, A.E. Becker, Circulation 103 (2001) 1955.
[65] A.D. Watson, N. Leitinger, M. Navab, K.F. Faull, S. Horkko, J.L. Witztum, W. Palinski, D. Schwenke, R.G. Salomon, W. Sha, G. Subbanagounder, A.M. Fogelman, J.A. Berliner, J. Biol. Chem. 272 (1997) 13597.
[66] J.H. Lee, J.S. Yang, S.H. Lee, M.H. Moon, J. Chromatogr. B Analyt. Technol. Biomed Life Sci. 1099 (2018) 56.
[67] N. Aiyar, J. Disa, Z. Ao, H. Ju, S. Nerurkar, R.N. Willette, C.H. Macphee, D.G. Johns, S.A. Douglas, Mol. Cell. Biochem. 295 (2007) 113.
[68] M. Calderon-Santiago, F. Priego-Capote, J.G. Galache-Osuna, M.D. Luque de Castro, J. Chromatogr. A 1371 (2014) 154.
[69] S.H. Kim, J.S. Yang, J.C. Lee, J.Y. Lee, J.Y. Lee, E. Kim, M.H. Moon, J. Chromatogr. A 1568 (2018) 91.
[70] I. Grundke-Iqbal, K. Iqbal, M. Quinlan, Y.C. Tung, M.S. Zaidi, H.M. Wisniewski, J. Biol. Chem. 261 (1986) 6084.
[71] J.J. Palop, L. Mucke, Nat. Neurosci. 13 (2010) 812.
[72] B.A. Yankner, Nat. Med. 2 (1996) 850.
[73] R.C. Petersen, R. Doody, A. Kurz, R.C. Mohs, J.C. Morris, P.V. Rabins, K. Ritchie, M. Rossor, L. Thal, B. Winblad, Arch. Neurol. 58 (2001) 1985.
[74] K.H. Kim, M.H. Moon, Anal. Chem. 83 (2011) 8652.
[75] K.H. Kim, J.Y. Lee, S. Lim, M.H. Moon, J. Chromatogr. A 1280 (2013) 92.
[76] I. Yang, K.H. Kim, J.Y. Lee, M.H. Moon, J. Chromatogr. A 1324 (2014) 224.
[77] Y. Lu, N. Yeung, N. Sieracki, N.M. Marshall, Nature 460 (2009) 855.
[78] G. Eskici, P.H. Axelsen, Biochemistry 51 (2012) 6289.
[79] N. Fatemi, B. Sarkar, J. Bioenerg. Biomembr. 34 (2002) 339.
[80] N. Stadler, R.A. Lindner, M.J. Davies, Arterioscler. Thromb. Vasc. Biol. 24 (2004) 949.
[81] J.Y. Kim, H.B. Lim, M.H. Moon, Anal. Chem. 88 (2016) 10198.